

Cite this: *Dalton Trans.*, 2011, **40**, 2038

www.rsc.org/dalton

PAPER

Electronic and photophysical properties of adducts of $[\text{Ru}(\text{bpy})_3]^{2+}$ and Dawson-type sulfite polyoxomolybdates $\alpha/\beta\text{-}[\text{Mo}_{18}\text{O}_{54}(\text{SO}_3)_2]^{4-}$ †

James J. Walsh,^a De-Liang Long,^b Leroy Cronin,^b Alan M. Bond,^c Robert J. Forster^a and Tia E. Keyes^{*a}

Received 4th November 2010, Accepted 23rd December 2010

DOI: 10.1039/c0dt01540g

The spectroscopic and photophysical properties of $[\text{Ru}(\text{bpy})_3]_2[\text{Mo}_{18}\text{O}_{54}(\text{SO}_3)_2]$, where bpy is 2,2'-bipyridyl and $[\text{Mo}_{18}\text{O}_{54}(\text{SO}_3)_2]^{4-}$ is either the α or β -sulfite containing polyoxomolybdate isomer, have been measured and compared with those for the well known but structurally distinct sulfate analogue, $\alpha\text{-}[\text{Mo}_{18}\text{O}_{54}(\text{SO}_4)_2]^{4-}$. Electronic difference spectroscopy revealed the presence of new spectral features around 480 nm, although they are weak in comparison with the $[\text{Ru}(\text{bpy})_3]_2[\text{Mo}_{18}\text{O}_{54}(\text{SO}_4)_2]$ analogue. Surprisingly, Stern–Volmer plots of $[\text{Ru}(\text{bpy})_3]^{2+}$ luminescence quenching by the polyoxometallate revealed the presence of both static and dynamic quenching for both α and $\beta\text{-}[\text{Mo}_{18}\text{O}_{54}(\text{SO}_3)_2]^{4-}$. The association constant inferred for the ion cluster $[\text{Ru}(\text{bpy})_3]_2\alpha\text{-}[\text{Mo}_{18}\text{O}_{54}(\text{SO}_4)_2]$ is $K = 5.9 \pm 0.56 \times 10^6$ and that for $[\text{Ru}(\text{bpy})_3]_2\beta\text{-}[\text{Mo}_{18}\text{O}_{54}(\text{SO}_4)_2]$ is $K = 1.0 \pm 0.09 \times 10^7$. Unlike the sulfate polyoxometalates, both sulfite polyoxometalate–ruthenium adducts are non-luminescent. Despite the strong electrostatic association in the adducts resonance Raman and photoelectrochemical studies suggests that unlike the sulfato polyoxometalate analogue there is no sensitization of the polyoxometalate photochemistry by the ruthenium centre for the sulfite anions. In addition, the adducts exhibit photochemical lability in acetonitrile, attributable to decomposition of the ruthenium complex, which has not been observed for other $[\text{Ru}(\text{bpy})_3]^{2+}$ -polyoxometalate adducts. These observations suggest that less electronic communication exists between the $[\text{Ru}(\text{bpy})_3]^{2+}$ and the sulfite polyoxoanions relative to their sulfate polyoxoanion counterparts, despite their structural and electronic analogy. The main distinction between sulfate and sulfite polyoxometalates lies in their reversible reduction potentials, which are more positive by approximately 100 mV for the sulfite anions. This suggests that the capacity for $[\text{Ru}(\text{bpy})_3]^{2+}$ or analogues to sensitize photoreduction in the adducts of polyoxometalates requires very sensitive redox tuning.

Introduction

Polyoxometalates (POMs) are an important and structurally diverse class of inorganic clusters which have found application across a broad range of disciplines including photocatalysis,¹ medicine,² and organic synthesis.³ In the field of photocatalysis, the Dawson polyoxometalate anions (see Fig. 1) are well known as efficient photocatalysts and are capable of multiple proton coupled redox processes. However, a key limitation is that in their fully oxidised state Dawson polyanions typically only absorb in the UV spectral region restricting their potential use in photovoltaic devices. An attractive but challenging proposition is to sensitize

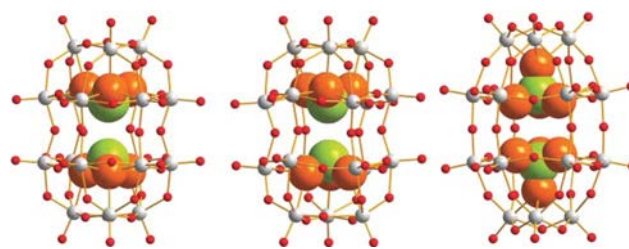


Fig. 1 Structures of the $\alpha\text{-SO}_3$ (left), $\beta\text{-SO}_3$ (centre) and $\alpha\text{-SO}_4$ -based (right) polyoxomolybdate clusters. The encapsulated sulfate and sulfite moieties are not to scale. Reproduced from ref. 15.

the polyoxometalate light-induced redox processes using a visible absorbing species that is strongly electronically coupled to the polyoxometalate and this has been the focus of recent research by our group and others.^{6–10}

As a result of their well-behaved and predictable redox and photophysical characteristics, $[\text{Ru}(\text{bpy})_3]^{2+}$ and its analogues have been widely applied as photosensitizers in interfacial photovoltaics

^aSchool of Chemical Sciences, National Centre for Sensor Research, Dublin City University, Glasnevin, Dublin, 9, Ireland. E-mail: tia.keyes@dcu.ie

^bWestCHEM, Department of Chemistry, The University of Glasgow, Glasgow, UK G12 8QQ. E-mail: L.Cronin@chem.gla.ac.uk

^cSchool of Chemistry, Monash University, Clayton, Victoria, 3800, Australia. E-mail: alan.bond@sci.monash.edu.au

† Electronic supplementary information (ESI) available: Fig. S1–S9. See DOI: 10.1039/c0dt01540g

and in supramolecular systems.¹⁹ It was therefore rationalized that they may be useful as sensitizers for polyoxometalate photochemistry as the cationic charge of most ruthenium polypyridyl complexes permits ready association with these anions.¹⁶ This has been exploited both in interfacial assemblies and in solution. For example, multilayers of a number of polyoxo anions and ruthenium and osmium polypyridyl complexes have been formed electrostatically on both glassy carbon and ITO (indium tin oxide) electrodes.^{4,1} In addition, it has been demonstrated that $[\text{Ru}(\text{bpy})_3]^{2+}$ forms stable electrostatic adducts with the non-reduced Dawson sulfato anions $[\text{M}_{18}\text{O}_{54}(\text{SO}_4)_2]^{4-}$ (where $\text{M} = \text{Mo}, \text{W}$) to form analytically pure $[\text{Ru}(\text{bpy})_3]_2[\text{M}_{18}\text{O}_{54}(\text{SO}_4)_2]$ adducts.⁵⁻⁹

The photophysics of the adducts $[\text{Ru}(\text{bpy})_3]_2[\text{M}_{18}\text{O}_{54}(\text{SO}_4)_2]$ (where $\text{M} = \text{Mo}, \text{W}$) have been thoroughly investigated.⁶⁻¹⁰ These species exhibited a remarkable degree of electronic coupling between the molybdate polyoxoanion and $[\text{Ru}(\text{bpy})_3]^{2+}$. This was reflected in the substantial photochemical stability conferred on the $[\text{Ru}(\text{bpy})_3]^{2+}$ cation when incorporated into the adduct; and the presence of a new optical transition, assigned as an intramolecular charge-transfer transition from resonance Raman spectroscopy, involving both the polyoxoanion and the $[\text{Ru}(\text{bpy})_3]^{2+}$ centres. Remarkably, this new cluster complex was luminescent.⁶ Comparable interactions were also observed between the tungsten analogue $[\text{W}_{18}\text{O}_{54}(\text{SO}_4)_2]^{4-}$ and $[\text{Ru}(\text{bpy})_3]^{2+}$.⁷ A photochemical study of $[\text{Ru}(\text{bpy})_3]_2[\text{M}_{18}\text{O}_{54}(\text{SO}_4)_2]$ ($\text{M} = \text{Mo}, \text{W}$) demonstrated that the quantum yield of $[\text{Ru}(\text{bpy})_3]_2[\text{M}_{18}\text{O}_{54}(\text{SO}_4)_2]$ photoreduction at 420 nm was an order of magnitude higher than that for $[\text{Hex}_4\text{N}]_4[\text{M}_{18}\text{O}_{54}(\text{SO}_4)_2]$ (Hex_4N is tetrahexylammonium) in the presence of benzyl alcohol substrate.⁸

The photophysics of ion clusters comprising $[\text{Ru}(\text{bpy})_3]^{2+}$ and lacunary substituted Dawson polyoxotungstates have also been investigated. Seery *et al.* demonstrated that the overall charge of the POM is not the only parameter driving ion-pair formation, as the association constant of $[\text{Ru}(\text{bpy})_3]_5[\text{P}_2\text{W}_{17}\text{O}_{61}]$ was orders of magnitude smaller than those for the lacunary substituted clusters $[\text{Ru}(\text{bpy})_3]_{3.5}[\text{P}_2\text{W}_{17}\text{O}_{61}(\text{Fe}^{3+}\cdot\text{OH}^-)]$ and $[\text{Ru}(\text{bpy})_3]_3[\text{P}_2\text{W}_{17}\text{O}_{61}(\text{Fe}^{3+}\text{Br}^-)]$.⁹ The photophysics of adducts of lacunary $[\text{P}_2\text{W}_{17}\text{O}_{61}(\text{Fe}^{3+}\text{OH}^-)]^{7-}$ ion and its unsubstituted parent ion $[\text{P}_2\text{W}_{18}\text{O}_{62}]^{6-}$ has also been investigated with $[\text{Ru}(\text{bpy})_2(\text{Mebpy-py})]^{2+}$.¹⁰ It was found that the bulkier Mebpy-py ligand had reduced the capacity for quenching by the polyoxotungstates, indicating that steric effects may be an important parameter in determining polyoxometalate ruthenium sensitizer interactions.

In this present contribution, the photophysical properties of $[\text{Ru}(\text{bpy})_3]^{2+}$ in the presence of the sulfite-containing Dawson-like anions $\alpha/\beta\text{-}[\text{Mo}_{18}\text{O}_{54}(\text{SO}_3)_2]^{4-}$ ($\alpha/\beta\text{-SO}_3$ POM) are presented. These relatively new structures were first reported in 2004.¹¹ The replacement of conventional sulfate groups with sulfite groups allows for the possibility of intramolecular electronic communication between the encapsulated sulfur atoms, and indeed the $\alpha\text{-SO}_3\text{-POM}$ is more difficult to reduce than the corresponding $\alpha\text{-}[\text{Mo}_{18}\text{O}_{54}(\text{SO}_4)_2]^{4-}$ ($\text{SO}_4\text{-POM}$) by about 100 mV.¹² The unusual distribution of charge within the metal oxide framework results in a distortion of the geometry from the standard Dawson anion to the non-conventional ‘‘peanut’’ configuration, which has also been observed in the non-reduced sulfite polyoxotungstate $\alpha\text{-}[\text{W}_{18}\text{O}_{54}(\text{SO}_3)_2]^{4-}$ and in the tin-substituted $[\text{H}_3\text{SnW}_{18}\text{O}_{60}]^{7-}$.^{13,14} The sulfite- and sulfate-containing species exhibit similar spectroscopic properties. The structures of $\alpha\text{-}[\text{Mo}_{18}\text{O}_{54}(\text{SO}_3)_2]^{4-}$, $\beta\text{-}$

$[\text{Mo}_{18}\text{O}_{54}(\text{SO}_3)_2]^{4-}$ and $\alpha\text{-}[\text{Mo}_{18}\text{O}_{54}(\text{SO}_4)_2]^{4-}$ are provided in Fig. 1 for comparison.

Although the $[\text{Ru}(\text{bpy})_3]^{2+}$ adducts of α and $\beta\text{-}[\text{Mo}_{18}\text{O}_{54}(\text{SO}_3)_2]^{4-}$ have been recently isolated, the spectroscopy and photophysics of these materials have not been studied to date.²⁰ The aim of this study, in the context of optimising ruthenium polyoxometalate interactions for sensitized photocatalysis, was to determine how the electronic properties, charge and isomeric structure of these materials influenced their interactions with the $[\text{Ru}(\text{bpy})_3]^{2+}$ sensitizer. Given the improved photocatalysis evident for the anions $\alpha/\beta\text{-}[\text{Mo}_{18}\text{O}_{54}(\text{SO}_3)_2]^{4-}$ by comparison with their sulfate analogue (see ESI[†]) a key objective is to determine if these properties extend to the $[\text{Ru}(\text{bpy})_3]^{2+}$ polyoxometalate adducts.

Experimental

Materials

Photophysical studies were carried out in aerated spectroscopic grade acetonitrile, dried over activated molecular sieves (3 Å) (Aldrich). Benzyl alcohol (spectroscopic grade, Aldrich) was dried over molecular sieves before use. $[\text{Ru}(\text{bpy})_3](\text{PF}_6)_2$ was synthesized as described previously.³⁰ $[\text{Pn}_4\text{N}]_4\alpha/\beta\text{-}[\text{Mo}_{18}\text{O}_{54}(\text{SO}_3)_2]$ (Pn_4N is tetrapentylammonium), $[\text{Hex}_4\text{N}]_4[\text{Mo}_{18}\text{O}_{54}(\text{SO}_4)_2]$, and $[\text{Ru}(\text{bpy})_3]_2\alpha/\beta\text{-}[\text{Mo}_{18}\text{O}_{54}(\text{SO}_3)_2]$ were synthesised according to literature methods and chemical analyses confirmed the compositions.^{11,18,20} Tetrabutylammonium tetrafluoroborate, lithium perchlorate and tetrabutylammonium hexafluorophosphate (Aldrich) were used as purchased. Potassium bromide (Riedel de Haen) was heated to 100 °C overnight, to remove residual water content. Ludox AM-30 was used as purchased (Aldrich). SiO_2 -coated ITO electrodes were used as purchased (Delta Technologies Ltd., Stillwater, MN, USA).

Methods

UV/Vis absorption spectra were obtained using a Varian Cary UV 50 Scan spectrophotometer. Steady state emission measurements were undertaken using a Cary Eclipse Fluorescence spectrometer with 10 nm emission and 10 nm excitation slits exciting at 450 nm. Time-correlated single photon counting (TCSPC) measurements were carried out using a Picoquant ‘Fluotime 100’ compact fluorescence lifetime spectrometer. The 450 nm pulse was generated by Picoquant ‘PDL 800-B’ pulsed diode laser and a Thurlby Thandar Instruments (TTi) TGP110 10 MHz pulse generator. An average of three measurements was taken for each sample, and the data was fitted to a monoexponential model using a reconvolution function. The instrument response function was measured using a scattering Ludox AM-30 colloidal silica solution. Resonance Raman spectra were collected on a Horiba Jobin Yvon HR800 UV spectrometer. The laser lines were generated by a Coherent Innova 70c tuneable Ar-ion laser (457.9, 488, 514.5 nm). A 10× microscope objective was used to focus the laser beam onto a sample ground into a compressed KBr disc or in acetonitrile solution. A 600 lines per mm diffraction grating was employed. The x -axis was calibrated *versus* the Rayleigh line (0 nm) and the phonon mode from silicon wafer (520 cm^{-1}). Attenuated total reflectance Fourier-Transform infrared (ATR-FTIR) spectroscopy was performed using a Varian 610-IR FTIR

microscope and a slide-on ATR accessory with a germanium crystal tip. The solid samples were mounted on a clean gold substrate and each spectrum acquired consisted of an average of 256 scans. Photoelectrochemical measurements were carried out using a standard three-electrode system and a CH Instruments 720b electrochemical workstation. The working electrodes were prepared by drop-casting 25 μl of concentrated (1 mM) acetonitrile suspension/solution of the metallo-adduct onto an ITO working electrode and allowing it to dry in air. A large area Pt flag was used as the counter electrode. An Ag wire was employed as the pseudo-reference, which was calibrated *versus* the IUPAC recommended ferrocene (Fc/Fc^+) internal reference. The potential was maintained constant at 400 mV throughout the experiment. Neat benzyl alcohol was used as both the solution and sacrificial donor; and no electrolyte was added so as to avoid ion-pair disruption. The light source for photochemistry was an Oriel 68811 arc lamp employing a 350 W Xe bulb and a >400 nm long pass filter, and was kept at a distance of 10 cm from the sample solution. The optical filter was purchased from Spectrogon UK Ltd.

Results and discussion

Absorption spectroscopy

Strong electronic communication between $[\text{Ru}(\text{bpy})_3]^{2+}$ and polyoxometalate is accompanied by significant modification to the UV/Vis spectroscopy of both species.^{6,7,8} In order to elucidate the presence of any new optical transitions resulting from the electronic interaction between α or β - $[\text{Mo}_{18}\text{O}_{54}(\text{SO}_3)_2]^{4-}$ and $[\text{Ru}(\text{bpy})_3]^{2+}$, difference electronic spectroscopy was used. In this approach, a range of solutions were prepared to investigate the effects of varying polyoxometalate concentration on the spectroscopy of a constant concentration of $[\text{Ru}(\text{bpy})_3]^{2+}$. Each solution contained 7.3×10^{-6} M $[\text{Ru}(\text{bpy})_3]^{2+}$ in which the concentration of α or β - $[\text{Mo}_{18}\text{O}_{54}(\text{SO}_3)_2]^{4-}$ was varied between 1×10^{-6} M and 3.0×10^{-5} M in order that the ratio of α or β - $[\text{Mo}_{18}\text{O}_{54}(\text{SO}_3)_2]^{4-}$ to $[\text{Ru}(\text{bpy})_3]^{2+}$ encompassed the 1:1 and 2:1 range. Fig. 2(a) shows the resulting electronic difference spectra generated by subtracting the electronically combined spectra of separate solutions of $[\text{Ru}(\text{bpy})_3]^{2+}$ (7.3×10^{-6} M) and, in this instance α - $[\text{Mo}_{18}\text{O}_{54}(\text{SO}_3)_2]^{4-}$ at its different concentrations from the actual spectra of the mixtures. Fig. 2(a) shows that titration of the polyoxometalate into the ruthenium solution resulted in a blue shift and reduction in intensity of a feature centred around 280 nm to approximately 260 nm, and the appearance of broad, weak features at approximately 320 nm and 475 nm.

These changes are similar to those reported previously for association of $[\text{Ru}(\text{bpy})_3]^{2+}$ with the sulfato polyoxometalate, although the extinction coefficient for the new band is approximately 50% weaker in the present case.^{6,7,9} Interestingly, unlike the sulfato species, when the ratio of $[\text{Ru}(\text{bpy})_3]^{2+}$ to α - $[\text{Mo}_{18}\text{O}_{54}(\text{SO}_3)_2]^{4-}$ decreased below 3:1 the λ_{max} of the new absorbance band shifted to approximately 485 nm. A feature around 380 nm also appeared at higher polyoxometalate concentrations, which was also observed when the sulfate polyoxoanion was used.⁶ As the polyoxometalate was added to $[\text{Ru}(\text{bpy})_3]^{2+}$, the ruthenium complex is initially present in significant excess, so the 2:1 associated species $[\text{Ru}(\text{bpy})_3]_2\alpha$ - $[\text{Mo}_{18}\text{O}_{54}(\text{SO}_3)_2]$ is predicted to

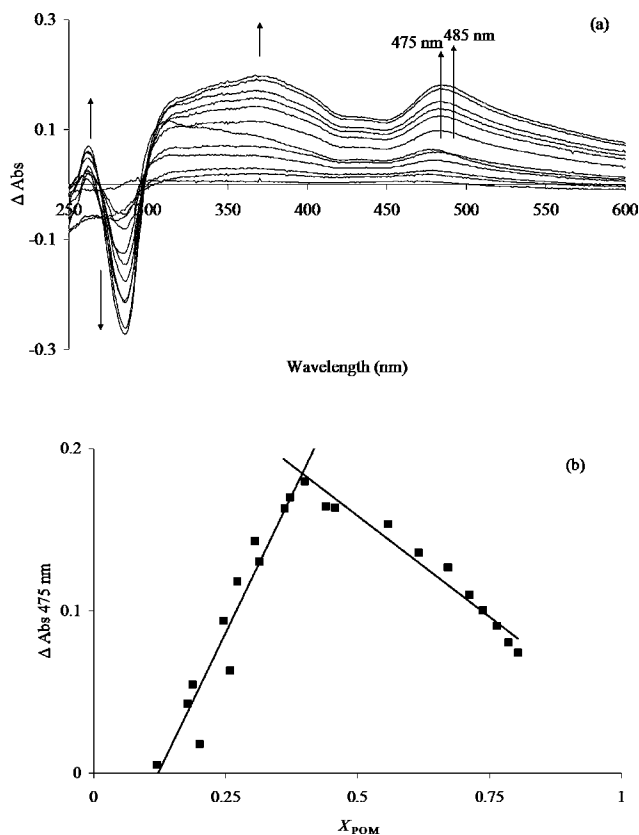


Fig. 2 (a) UV/Vis difference spectra of $[\text{Ru}(\text{bpy})_3]^{2+}$ (7.3×10^{-6} M) upon addition of α - $[\text{Mo}_{18}\text{O}_{54}(\text{SO}_3)_2]^{4-}$ (9.9×10^{-7} M to 4.8×10^{-6} M) in dry acetonitrile. (b) Job's plot of absorbance change at 475 nm as a function of α - $[\text{Mo}_{18}\text{O}_{54}(\text{SO}_3)_2]^{4-}$ concentration.

form first. Consequently, the higher energy feature is likely to arise from the 2:1 complex.

Fig. 2(b) shows a Job's plot constructed from the growth of the feature at 475 nm. The maximum of the Job's plot occurred at a polyoxometalate mole fraction (X_{POM}) of approximately 0.375, which corresponds to a α - $[\text{Mo}_{18}\text{O}_{54}(\text{SO}_3)_2]^{4-}$ to $[\text{Ru}(\text{bpy})_3]^{2+}$ ratio of approximately 0.6:1. This is in good agreement with the expected value of 0.5:1 ($X_{\text{POM}} = 0.33$) for a complex where the anionic charge on the polyoxometalate is fully compensated for by the dicationic ruthenium complex. When the corresponding isomer β - $[\text{Mo}_{18}\text{O}_{54}(\text{SO}_3)_2]^{4-}$ was investigated similar behaviour was observed, although the new visible absorbance grew at 479 nm and shifted to 486 nm upon reaching X_{POM} of 0.29, which again, is close to the expected value of 0.33. These data strongly indicate that $[\text{Ru}(\text{bpy})_3]^{2+}$ associates electrostatically with α/β - $[\text{Mo}_{18}\text{O}_{54}(\text{SO}_3)_2]^{4-}$ in a 2:1 ratio in acetonitrile.

The ATR-FTIR spectra of the POMs and their Ru metallo-adducts were obtained (ESI†) to identify any structural changes induced in the complexes on association. Modes characteristic of the polyoxomolybdate anion are shifted by between 3 and 8 cm^{-1} by comparison with the parent anion. For the composite material, polyoxomolybdate modes are observed at 781 cm^{-1} (Mo–O–Mo involving edge-sharing octahedral), 972 cm^{-1} (Mo–O–Mo involving corner-sharing octahedral) and 935 cm^{-1} (Mo=O terminal mode).^{21,22} The sulfite S=O symmetric stretch was observed at 902 cm^{-1} .^{21,23} Interestingly, the metal-oxide stretch at

781 cm⁻¹ and the out-of-plane C–H bending at 757 cm⁻¹ shift to lower and higher energy, respectively, upon association relative to their parent ion spectra; while the bipyridine out-of-plane ring bending at 730 cm⁻¹ is unaffected.^{24,25} Comparable behaviour has been reported in several other Ru-POM hybrid systems and indicates strong association.^{26,27} Peaks between 1350 and 1500 cm⁻¹ were attributed to the tetrapentylammonium counterion, and the Ru complex PF₆⁻ counterion was observed at 835 cm⁻¹ for the parent ions. None of these modes are present in the composite material spectrum, indicating, in agreement with the Job's plot, that full ion compensation between cation and anion occurs.

Luminescence studies. In order to determine the impact of association of [Mo₁₈O₅₄(SO₃)₂]⁴⁺ on the photophysical properties of [Ru(bpy)₃]²⁺, the luminescence of this complex was studied as a function of polyoxometalate concentration in dry acetonitrile.

Fig. 3 shows that significant quenching of the [Ru(bpy)₃]²⁺ MLCT luminescence is observed upon addition of α-[Mo₁₈O₅₄(SO₃)₂]⁴⁺. The [Ru(bpy)₃]²⁺ phosphorescence centred at 610 nm decreased steadily upon addition of successive quantities of α-[Mo₁₈O₅₄(SO₃)₂]⁴⁺ or β-[Mo₁₈O₅₄(SO₃)₂]⁴⁺ as the ions associated, although there was no evidence for a shift in the luminescence λ_{max}. This behaviour contrasts with that of the sulfato polyoxomolybdate [Mo₁₈O₅₄(SO₄)₂]⁴⁺, where significant changes in the emission maxima and peak shape were evident. A shoulder observed at ~630 nm was attributed to luminescence from the 2:1 associated complex.⁶ Even though a very weak residual luminescence at 610 nm remains when the α/β-[Mo₁₈O₅₄(SO₃)₂]⁴⁺ concentration exceeds that of the ruthenium complex by more than 2.5 times, it is likely that this emission arises from unassociated [Ru(bpy)₃]²⁺ rather than an intrinsic emission from the associated complex. To verify this, the isolated solids [Ru(bpy)₃]₂α/β-[Mo₁₈O₅₄(SO₃)₂] were examined using confocal fluorescence microscopy which confirmed that the 2:1 complex is non-emissive in the solid state. The excitation spectra taken for the weak residual emission of the solution species confirmed that it matched that of [Ru(bpy)₃]²⁺ suggesting that the any remaining emission arises from unassociated [Ru(bpy)₃]²⁺.

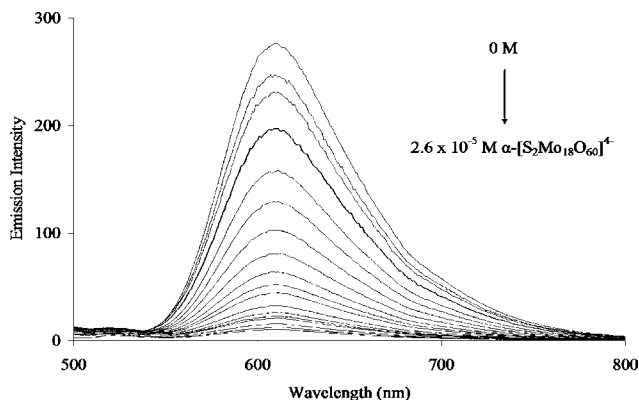


Fig. 3 Luminescence quenching of [Ru(bpy)₃]²⁺ (1.0 × 10⁻⁵ M) by addition of the polyoxometalate α-[Mo₁₈O₅₄(SO₃)₂]⁴⁺ (1.6 × 10⁻⁶ M to 2.6 × 10⁻⁵ M) in dry MeCN.

Comparison of the behaviour of the luminescence intensity and lifetime of [Ru(bpy)₃]²⁺ as a function of the quencher concentration

can yield insights into the nature of the interaction between the two compounds. Dynamic quenching, where interaction between the species is collisional and therefore diffusion controlled, is expected to follow the Stern–Volmer equation (eqn (1)):

$$\frac{I_0}{I} \text{ or } \frac{\tau_0}{\tau} \text{ or } \frac{\Phi_0}{\Phi} = 1 + K_{SV}[Q] \quad (1)$$

where [Q] is the concentration of the quencher; *I* is the luminescence intensity; τ is the luminescent lifetime of the luminophore; and Φ is the luminescence quantum yield. *K*_{SV} is the Stern–Volmer constant (eqn (2)):

$$K_{SV} = k_q \times \tau_0 \quad (2)$$

where *k*_q is the experimental rate constant for quenching and τ_0 is the lifetime of the unquenched fluorophore. For purely static quenching, where a non-luminescent association complex forms between the complex an analogous equation is employed (eqn (3)), but the slope is now the association constant, *K*.

$$\frac{I_0}{I} = 1 + K[Q] \quad (3)$$

In the case of purely static quenching, leading to a non-emitting association complex, the observed lifetime of the luminophore is expected to be unaffected by quencher concentration, so the *I*₀/*I* or Φ_0/Φ plots vary with quencher concentration but τ_0/τ does not. In a mixed static and dynamic scenario, the lifetime will be affected by quencher concentration, but the slopes of the *I*₀/*I* plot and τ_0/τ plots differ. Consequently, comparison of the luminescence lifetime and intensity as a function of quencher concentration can be used to assess whether quenching is static, dynamic or a combination of both. The *I*₀/*I* plot and τ_0/τ plots for addition of the sulfite polyoxomolybdates to [Ru(bpy)₃]²⁺ are shown in Fig. 4 and 5.

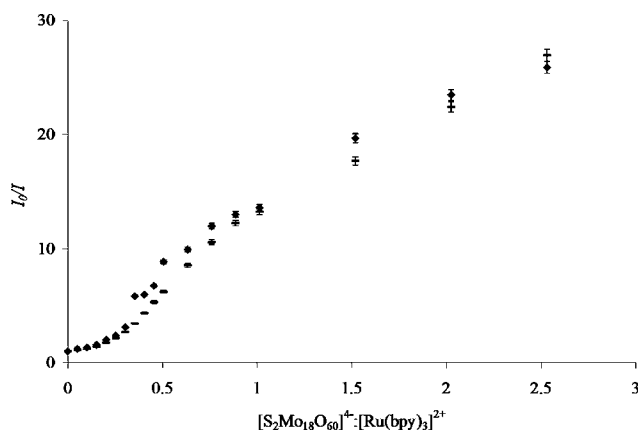
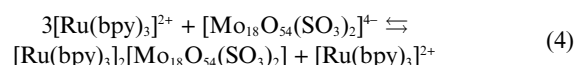


Fig. 4 Stern–Volmer plots of the emission quenching of [Ru(bpy)₃]²⁺ (1.0 × 10⁻⁵ M) by α-[Mo₁₈O₅₄(SO₃)₂]⁴⁺ (—) and β-[Mo₁₈O₅₄(SO₃)₂]⁴⁺ (◆) (1.6 × 10⁻⁶ M to 2.6 × 10⁻⁵ M) in aerated acetonitrile.

It is perhaps important to remember that the luminophore, [Ru(bpy)₃]²⁺, is present in excess at the beginning of the experiment and that the formation of the associated complex most likely occurs in the following sequence:



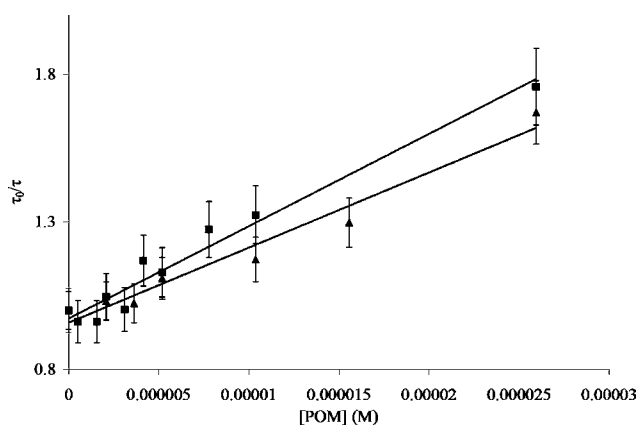


Fig. 5 Luminescent lifetime Stern–Volmer plots of 5.0×10^{-6} M $[\text{Ru}(\text{bpy})_3]^{2+}$ lifetime quenched by α - $[\text{Mo}_{18}\text{O}_{54}(\text{SO}_3)_2]^{4-}$ (■) and by β - $[\text{Mo}_{18}\text{O}_{54}(\text{SO}_3)_2]^{4-}$ (▲) in MeCN.

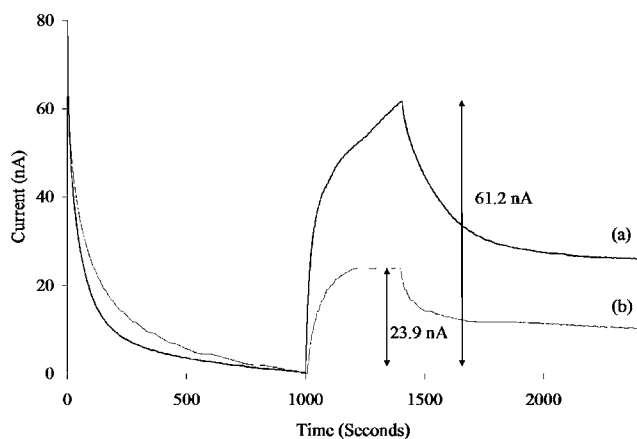
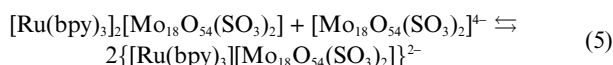


Fig. 6 Photocurrents generated by (a) $[(\text{Pn})_4\text{N}]_4\alpha$ - $[\text{Mo}_{18}\text{O}_{54}(\text{SO}_3)_2]$ and (b) $[\text{Ru}(\text{bpy})_3]_2\alpha$ - $[\text{Mo}_{18}\text{O}_{54}(\text{SO}_3)_2]$ modified ITO electrodes in contact with benzyl alcohol (baselines normalized). Each sample was irradiated for 400 s by light from a 300 W Xe arc lamp with a >400 nm long pass filter (light on 1000 s, light off 1400 s).



Initially, when the ruthenium complex is present in large excess, the 2 : 1 complex would be expected to form. As shown in Fig. 4, the data is non-linear with significant upward curvature and at least two distinct regions of response, when applied to a Stern–Volmer model, one explanation for such behaviour is that the 2 : 1 adduct remains luminescent but the 1 : 1 is not. However, as described above, fluorescence microscopy confirmed this is not the case (ESI†). Upward curvature in the Stern–Volmer plot is typical in situations where the quencher can both associate with the luminophore and quench it through molecular collision (*i.e.*: mixed static and dynamic quenching).²⁹ Because of the electrostatic nature of the interaction between the ruthenium and polyoxometalate centres purely static quenching was anticipated.

Time-resolved luminescence. To investigate the non-linearity of the luminescence intensity data when applied to the Stern–Volmer

model, time-correlated single photon counting was employed to study the effect of increasing polyoxometalate concentration on the luminescent lifetime of $[\text{Ru}(\text{bpy})_3]^{2+}$ in MeCN. The data obtained are shown in Fig. 5.

As data derived from electronic spectroscopy indicated, a 2 : 1 complex forms between ruthenium and polyoxometalate in MeCN and, on the basis of previous studies, it was expected that the quenching would be purely static. However, surprisingly as shown in Fig. 5 where the lifetime data was applied to a Stern–Volmer plot, *i.e.* τ_0/τ versus $[\text{Q}]$, for both sulfite isomers, a reduction in $[\text{Ru}(\text{bpy})_3]^{2+}$ lifetime was found to accompany increasing polyoxometalate concentration. In each case, the lifetime fits remained monoexponential. This implies that there is a dynamic component to the quenching of the ruthenium by both sulfite polyoxometalates. The slopes of τ_0/τ versus $[\text{Q}]$ are equal to K_{SV} , according to eqn (1) which are $3.1 \times 10^4 \text{ mol}^{-1}$ for α - $[\text{Mo}_{18}\text{O}_{54}(\text{SO}_3)_2]^{4-}$ and $2.5 \times 10^4 \text{ mol}^{-1}$ for β - $[\text{Mo}_{18}\text{O}_{54}(\text{SO}_3)_2]^{4-}$ over the data range corresponding to a 2 : 1 $[\text{Ru}(\text{bpy})_3]^{2+} : [\text{Mo}_{18}\text{O}_{54}(\text{SO}_3)_2]^{4-}$ ratio. The dynamic quenching rate constants, k_{q} were estimated according to eqn (2) to be $1.6 \pm 0.2 \times 10^{11} \text{ L mol}^{-1} \text{ s}^{-1}$ and $1.9 \pm 0.10 \times 10^{11} \text{ L mol}^{-1} \text{ s}^{-1}$ for the α and β isomers respectively, these exceeded the diffusion controlled rate (approx. $10^{10} \text{ L mol}^{-1} \text{ s}^{-1}$) which is consistent with dynamic quenching which contains a static contribution.

A modified form of the emission Stern–Volmer eqn (6) can be used for mixed static and dynamic quenching,²⁹ the parameters are as explained above:

$$\frac{I_0}{I} = 1 + (K_{\text{SV}} + K_{\text{a}})[\text{Q}] + K_{\text{SV}}K_{\text{a}}[\text{Q}]^2 \quad (6)$$

Therefore, plotting $((I_0/I) - 1)/[\text{POM}]$ vs. $[\text{POM}]$ gave a plot with a slope equal to $K_{\text{SV}} \times K_{\text{a}}$. Since the K_{SV} values were obtained from lifetime data, K_{a} values were derived from these fits as $5.9 \pm 0.56 \times 10^6$ and $1.0 \pm 0.09 \times 10^7$ for the α and β isomers respectively (see ESI†). The K_{a} value obtained for the association of the corresponding 2 : 1 sulfate polyoxometalate complex with $[\text{Ru}(\text{bpy})_3]^{2+}$ was 1×10^6 ; this suggests the sulfite polyoxomolybdate analogue has a slightly higher affinity for $[\text{Ru}(\text{bpy})_3]^{2+}$ compared with sulfato.⁹ Importantly, these earlier studies indicated that the charge on the polyoxometalate was not solely responsible for the magnitude of the association constant with $[\text{Ru}(\text{bpy})_3]^{2+}$.

Influence of ion-pairing on adduct formation

To investigate the association between $[\text{Ru}(\text{bpy})_3]^{2+}$ and α - $[\text{Mo}_{18}\text{O}_{54}(\text{SO}_3)_2]^{4-}$ further, the effect of ionic strength on the associated cluster was examined by studying the luminescence recovery from $[\text{Ru}(\text{bpy})_3]^{2+}$ with increasing salt concentration. It is well known that ClO_4^- ions have a high propensity to ion-pair with ruthenium polypyridyl complexes, and this salt has been shown to disrupt ion pairing in the case of $[\text{Ru}(\text{bpy})_3]^{2+}$ and other Dawson polyoxometalates.^{6,7,9} The impact of LiClO_4 addition to a solution of $[\text{Ru}(\text{bpy})_3]_2\beta$ - $[\text{Mo}_{18}\text{O}_{54}(\text{SO}_3)_2]$ containing a ten-fold excess of polyoxometalate is shown in ESI.†

This study shows that by a concentration of $9.86 \times 10^{-3} \text{ M}$ LiClO_4 the luminescence of free $[\text{Ru}(\text{bpy})_3]^{2+}$ was fully recovered. A plot of recovering luminescence intensity as a function of increasing LiClO_4 concentration (see ESI†) exhibited upward curvature which was remarkably similar to that for the addition

of LiClO₄ to a solution of [P₂W₁₇O₆₁(FeOH₂)⁷⁻ and [Ru(bpy)₃]²⁺ recorded by Seery *et al.*, although the absolute concentrations used differ.⁹ Here a 75-fold excess of LiClO₄ over polyoxometalate was required to disrupt the ion–ion association.

The analogous experiment was then repeated with the α isomer. In this case, addition of LiClO₄ to a solution of 1×10^{-5} M [Ru(bpy)₃]²⁺ and 1×10^{-4} M α -[Mo₁₈O₅₄(SO₃)₂]⁴⁻ only resulted in partial recovery of the [Ru(bpy)₃]²⁺ luminescence, and at high LiClO₄ concentrations. A UV/Vis spectrum taken before and after the additions showed that the [Ru(bpy)₃]₂ α -[Mo₁₈O₅₄(SO₃)₂] MLCT at \sim 475 nm had also reduced dramatically in intensity, and the baseline had also shifted. This was attributed to poor solubility of the complex in acetonitrile which caused precipitation in the presence of the salt. This was also observed when TBA BF₄ or TBA PF₆ was employed. The origin of this difference in solubility observed for the two isomers is unknown as they are isoelectronic and isostructural.

Resonance Raman spectroscopy. The new absorbance formed around 475 nm in the UV-vis spectrum, on the basis of comparison with other clusters, is thought to arise from a new inter-metal charge-transfer within the cluster. In order to confirm this, resonance Raman spectroscopy was conducted of the isolated 2:1 adducts in KBr exciting at 488 nm, *i.e.* close to the new absorbance feature. In addition to the adducts, control spectra of the parent polyoxometalates complexes and [Ru(bpy)₃]²⁺, were collected under 488 nm excitation for comparison. The spectra are presented in ESI†. Spectral intensities are normalized for clarity; the two ruthenium containing complexes are expected to be resonant at 488 nm whereas [Pn₄N]₅ α -[Mo₁₈O₅₄(SO₃)₂] is not, so there are large differences in absolute Raman spectral intensity between the ruthenium-containing complexes and the parent polyoxometalate.

The Raman spectra of both parent sulfite polyoxometalates are similar although there are significant differences in the relative intensities of the modes. Common features for both isomers are the Mo–O stretch modes between 900 and 990 cm⁻¹. An Mo–O bending mode is also observed at 388 cm⁻¹.¹⁷ There are also some weak features associated with a small amount of reduced parent [Pn₄N]₅ α -[Mo₁₈O₅₄(SO₃)₂] in the range between 1400 cm⁻¹ and 1500 cm⁻¹. This was confirmed by examining the Raman spectrum of the isolated electroreduced polyanion (see ESI†). Their intensity is artificially high as this complex, which has an intense absorbance in the visible region, is resonantly enhanced at 488 nm. The ³MLCT resonance Raman spectrum of [Ru(bpy)₃]²⁺ is well known and exhibits signature modes at 1608, 1565, 1492, 1320, 1279, 1178, 1030 and 670 cm⁻¹, all attributed to bpy vibrations, and a Ru–N mode at 375 cm⁻¹.

The Raman spectra of the composite materials excited at 488 nm are shown in ESI.† A number of weak features are detected in the composite, that are not observed for [Ru(bpy)₃]²⁺ alone for the [Ru(bpy)₃]₂ α -[Mo₁₈O₅₄(SO₃)₂]⁴⁻, particularly the two modes at 1433 and 1467 cm⁻¹ these were attributed to a small amount of the reduced parent in the α isomer, which appear because of resonance with the MMCT transition of the reduced parent. Interestingly, though the prominent Mo–O asymmetric stretch mode which was resonantly enhanced in the sulfate polyoxometalate ruthenium adducts is not observed for either of the sulfite adducts studied here.^{6,7,9} This suggests that the 475 nm transition is either too

weak to provide a significant resonantly enhanced signal or that it is not in this instance an inter-metal transition. This observation is consistent with the spectroscopy above and suggests that the inter-complex electronic communication within the adduct for the sulfite polyoxomolybdates is considerably lower than for the sulfate analogues.

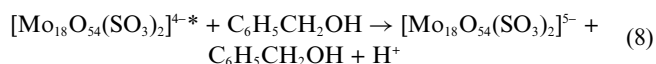
The [Ru(bpy)₃]²⁺ modes in the composite are affected by association with the polyoxometalate; they are broadened relative to their analogues in the parent ion. This is indicative of heterogeneity in the microenvironment experienced by the ruthenium centres when incorporated into an adduct. Spectra of the corresponding isomer β -[Mo₁₈O₅₄(SO₃)₂]⁴⁻ and its ruthenium adduct [Ru(bpy)₃]₂ β -[Mo₁₈O₅₄(SO₃)₂] were very similar to those of the α isomer. Overall, unlike the sulfato analogue, there was no evidence for resonantly enhanced Mo–O modes but significant broadening of the [Ru(bpy)₃]²⁺ modes were evident on its association with both polyoxometalates.

Photochemical stability. Previous studies have demonstrated that [Ru(bpy)₃]²⁺, normally quite photolabile in acetonitrile, becomes exceptionally photochemically stable when associated with a Dawson polyoxoanion.^{6,7,9} This was attributed to the strong electronic perturbation of the ruthenium centre by the polyoxometalate. Given the relatively weak electronic interaction indicated here between the sulfite polyoxomolybdates it is important to see if this influences the photostability of the [Ru(bpy)₃]²⁺ centre. Photochemical stability studies of the novel cluster complexes in acetonitrile were performed using a 300 W Xe arc lamp with a <400 nm optical cut-off filter. The impact of 4 h irradiation of approximately 1×10^{-5} M of [Ru(bpy)₃]₂ β -[Mo₁₈O₅₄(SO₃)₂], [Ru(bpy)₃]₂ β -[Mo₁₈O₅₄(SO₃)₂] and [Ru(bpy)₃]²⁺ in acetonitrile were compared. In each instance the samples were absorbance matched over the excitation window. Photochemically induced changes in the complexes were monitored by UV/Vis spectroscopy during the course of the photolysis. Over four hours of irradiation approximately 8% of the intensity of the [Ru(bpy)₃]²⁺ MLCT absorbance was lost for [Ru(bpy)₃]₂ β -[Mo₁₈O₅₄(SO₃)₂], compared with 18% from [Ru(bpy)₃]₂ α -[Mo₁₈O₅₄(SO₃)₂]. The photolability of the [Ru(bpy)₃]²⁺ cation in MeCN is well known,²⁸ and in comparison an absorbance matched ($\sim 1 \times 10^{-5}$ M) solution of [Ru(bpy)₃]²⁺ showed a decrease in MLCT absorbance of approximately 30%. Interestingly, for both sulfite polyoxometalates, the photostability of the complex had increased compared to the control. However comparison with the adduct of the sulfate analogue reveals that this complex exhibited no decomposition at the ruthenium centre under the same conditions. This is again consistent with reduced electronic interaction between the sulfite polyoxometalates and the ruthenium centre. As the ruthenium centre is non-luminescent when associated with the sulfite polyoxometalates, the origin of the modestly increased photostability of the ruthenium centre in the adduct may be kinetic, due to the reduced lifetime of the excited state of this centre. Attempts to measure the excited state lifetime of both [Ru(bpy)₃]₂ β -[Mo₁₈O₅₄(SO₃)₂] and [Ru(bpy)₃]₂ α -[Mo₁₈O₅₄(SO₃)₂] by transient spectroscopy showed that it was below 15 ns, the resolution of our instrument.

Photo-electrochemistry. The presence of an inter-complex charge-transfer transition in previous Dawson polymolybdate– and polytungstate–[Ru(bpy)₃]²⁺ adducts was implicated in the ability of the [Ru(bpy)₃]²⁺ unit to sensitize the photocatalytic activity

of these polyoxometalates. For example, for $[\text{Mo}_{18}\text{O}_{54}(\text{SO}_3)_2]^{4-}$ dissolved in DMF, the quantum yield of photocatalysis was increased substantially under visible irradiation in the presence of the ruthenium cation.⁸

Initial photoelectrochemical studies of $[(\text{Pn})_4\text{N}]_4\alpha\text{-}[\text{Mo}_{18}\text{O}_{54}(\text{SO}_3)_2]$ and $[\text{Ru}(\text{bpy})_3]_2\alpha\text{-}[\text{Mo}_{18}\text{O}_{54}(\text{SO}_3)_2]$ were carried out on an ITO electrode using benzyl alcohol as the donor. The samples were prepared by drop casting the composite onto the electrode. In the case of the pure polyoxometalate, a relatively uniform thin film was formed but the 2:1 Ru:POM layer did not deposit as evenly. The modified ITO electrode was immersed in benzyl alcohol and irradiated with >400 nm white light using a long pass filter. In order to ensure that the ion-pair remained associated, the photoelectrochemical experiments were performed in the absence of any added supporting electrolyte. The absence of electrolyte meant that IR drop is significant, nonetheless photocatalytic current could be observed. The potential was held at 0.4 V to ensure that following photoreduction of polyoxometalate by the benzyl alcohol (eqn (7) and (8)), the reduced polyoxometalate (eqn (8)) was reoxidised back to $[\text{Mo}_{18}\text{O}_{54}(\text{SO}_3)_2]^{4-}$ at the working electrode to generate photocatalytic current.



The results of this experiment, shown in Fig. 6, are striking in that both samples generate substantial photocurrents under irradiation with visible light. However, photocurrent generation by the polyoxometalate anion was disappointingly reduced by approximately 60% in the presence of $[\text{Ru}(\text{bpy})_3]^{2+}$ (reduction from 61.2 nA to 23.9 nA). The reduction in photocurrent confirms that in the case of the sulfite polyoxometalate, the ruthenium does not sensitize the polyoxometalate. The reduction of photocurrent in the presence ruthenium is attributed to the filtering of the incident light by the ruthenium absorbance. Comparison with the β -isomer revealed a slightly higher photocurrent (73.5 nA) for the parent, compared with the α form under identical conditions. The associated species, $[\text{Ru}(\text{bpy})_3]_2\beta\text{-}[\text{Mo}_{18}\text{O}_{54}(\text{SO}_3)_2]$, also generated a higher current than the α analogue, producing 52 nA at the electrode. Interestingly the reduction in current when the Ru was present was not as severe as in the α -isomer case (approximately a 30% decrease relative to 60% for the α experiments).

Conclusions

The photophysics of $[\text{Ru}(\text{bpy})_3]^{2+}$ in the presence of the Dawson-like polyoxomolybdates $\alpha\text{-}[\text{Mo}_{18}\text{O}_{54}(\text{SO}_3)_2]^{4-}$ and $\beta\text{-}[\text{Mo}_{18}\text{O}_{54}(\text{SO}_3)_2]^{4-}$ have been studied. Both anions associate strongly with $[\text{Ru}(\text{bpy})_3]^{2+}$ to form adducts which from UV-vis spectroscopy form with approximately 2:1 ratio Ru:POM. Surprisingly, unlike other $[\text{Ru}(\text{bpy})_3]^{2+}$ polyoxoanion studies, the quenching of the ruthenium excited state followed mixed static and dynamic behaviour. Difference electronic spectroscopy of the resulting adducts revealed the presence of a weak new electronic transition which was red-shifted with respect to the $[\text{Ru}(\text{bpy})_3]^{2+}$ ³MLCT centred at 450 nm which was weaker in

intensity and blue shifted compared to a similar absorbance in the sulfato anions. Resonance Raman spectroscopy, exciting into this new transition, did not show the anticipated resonantly enhanced Mo–O modes seen for the sulfato analogues which have been attributed to an inter-complex transition. Photo-electrochemical measurements on ITO electrodes with white light irradiation demonstrated that the associated $[\text{Ru}(\text{bpy})_3]_2\alpha\text{-}[\text{Mo}_{18}\text{O}_{54}(\text{SO}_3)_2]$, unlike the sulfate analogue $[\text{Pn}_4\text{N}]_4\alpha\text{-}[\text{Mo}_{18}\text{O}_{54}(\text{SO}_3)_2]$ does not sensitize photocatalytic oxidation of benzyl alcohol. Although the parent sulfite molybdate does exhibit a significantly greater photocurrent from photocatalytic oxidation of benzyl alcohol than the sulfato analogue.

Acknowledgements

This study was supported by the Australian Research Council and is based upon work supported by Science Foundation Ireland under award number 07/RFP/MASF386.

References

- 1 E. Papaconstantinou, *Chem. Soc. Rev.*, 1989, **18**, 1–31.
- 2 J. T. Rhule, C. L. Hill, D. A. Judd and R. F. Schinazi, *Chem. Rev.*, 1998, **98**, 327–357.
- 3 J. Das and K. M. Parida, *J. Mol. Catal. A: Chem.*, 2007, **264**, 248–254.
- 4 (a) A. Kuhn and F. Anson, *Langmuir*, 1996, **12**, 5481–5488; (b) L. Cheng and J. A. Cox, *Chem. Mater.*, 2002, **14**, 6; (c) H. Ma, T. Dong, F. Wang, W. Zhang and B. Zhou, *Electrochim. Acta*, 2006, **51**, 4965; (d) M. Zynek, M. Serantoni, S. Beloshapkin, E. Dempsey and T. McCormac, *Electroanalysis*, 2007, **19**, 681.
- 5 V. M. Hultgren, A. M. Bond and A. G. Wedd, *J. Chem. Soc., Dalton Trans.*, 2001, 1076–1082.
- 6 T. E. Keyes, E. Gicquel, L. Guerin, R. J. Forster, V. M. Hultgren, A. M. Bond and A. G. Wedd, *Inorg. Chem.*, 2003, **42**, 7897–7905.
- 7 M. K. Seery, L. Guerin, R. J. Forster, E. Gicquel, V. M. Hultgren, A. M. Bond, A. G. Wedd and T. E. Keyes, *J. Phys. Chem. A*, 2004, **108**, 7399–7405.
- 8 N. Fay, V. M. Hultgren, A. G. Wedd, T. E. Keyes, R. J. Forster, D. Leane and A. M. Bond, *Dalton Trans.*, 2006, 4218–4227.
- 9 M. K. Seery, N. Fay, T. McCormac, E. Dempsey, R. J. Forster and T. E. Keyes, *Phys. Chem. Chem. Phys.*, 2005, **7**, 3426–3433.
- 10 L. Ruhlmann, C. Costa-Coquelard, J. Hao, S. Jiang, C. He, L. Sun and I. Lampre, *Can. J. Chem.*, 2008, **86**, 1034–1043.
- 11 D-L. Long, P. K. Gerler and L. Cronin, *Angew. Chem., Int. Ed.*, 2004, **43**, 1817–1820.
- 12 C. Baffert, J. F. Boas, A. M. Bond, P. Kogerler, D-L. Long, J. R. Pilbrow and L. Cronin, *Chem.–Eur. J.*, 2006, **12**, 8472–8483.
- 13 D-L. Long, H. Abbas, P. Kogerler and L. Cronin, *Angew. Chem., Int. Ed.*, 2005, **44**, 3415–3419.
- 14 B. Krebs, E. Droste, M. Piepenbrink and G. Vollmer, *C. R. Acad. Sci. Ser. IIc: Chim.*, 2000, **3**, 205.
- 15 D-L. Long, E. Burkholder and L. Cronin, *Chem. Soc. Rev.*, 2007, **36**, 105–121.
- 16 R. Ballardini, M. T. Gandolfi and V. Balzani, *Inorg. Chem.*, 1987, **26**, 862–867.
- 17 L. Le Bihan, P. Blanchard, M. Fournier, J. Grimblot and E. Payen, *J. Chem. Soc., Faraday Trans.*, 1998, **94**, 937–940.
- 18 J. B. Cooper, D. M. Way, A. M. Bond and A. G. Wedd, *Inorg. Chem.*, 1993, **32**, 2416.
- 19 M. Gratzel, *Philos. Trans. R. Soc. London, Ser. A*, 2007, **365**, 993–1005.
- 20 M. Goral, T. McCormac, E. Dempsey, D-L. Long, L. Cronin and A. M. Bond, *Dalton Trans.*, 2009, 6727.
- 21 M. J. Manos, J. D. Woollins, A. M. Z. Slawin and T. A. Kabanos, *Angew. Chem., Int. Ed.*, 2002, **41**, 2801–2805.
- 22 D. M. Way, J. B. Cooper, M. Sadek, T. Vu, P. J. Mahon, A. M. Bond, R. T. C. Brownlee and A. G. Wedd, *Inorg. Chem.*, 1997, **36**, 4227–4233.

-
- 23 S. K. Verma and M. K. Deb, *J. Agric. Food Chem.*, 2007, **55**, 8319–8324.
- 24 R. M. Silverstein, and F. X. Webster, *Spectrometric Identification of Organic Compounds*, 6th edn, Wiley, p. 143.
- 25 P. K. Mallick, G. D. Danzer, D. P. Strommen and J. R. Kincaid, *J. Phys. Chem.*, 1988, **92**, 5628–5634.
- 26 Y. Li, H. Zhu and X. Yang, *Talanta*, 2009, **80**, 870–874.
- 27 L. Bi, H. Wang, Y. Shen, E. Wang and S. Dong, *Electrochem. Commun.*, 2003, **5**, 913–918.
- 28 B. Durham, J. V. Casper, J. K. Nagel and T. J. Meyer, *J. Am. Chem. Soc.*, 1982, **104**, 4803.
- 29 J. R. Lakowicz, *Principles of Fluorescence Spectroscopy*, 3rd edn, Springer, pp. 282–283.
- 30 R. A. Palmer and T. S. Piper, *Inorg. Chem.*, 1966, **5**, 864.